

Transport of multi-pollutant molecules in titanium-based nanopore with molecular dynamics

Qi Xin^{1,2,#}, Yang Yang^{1,2,#}, Shaojun Liu^{1,2}, Chenghang Zheng^{1,2}, Qingyang Lin^{1,2,*}, Xiang Gao^{1,2,*}

1 State Key Lab of Clean Energy Utilization, State Environmental Protection Center for Coal-Fired Air Pollution Control, Zhejiang University, Hangzhou, 310027, China

2 Jiaxing Research Institute of Zhejiang University, Jiaxing, 314001, China

These authors contributed equally to this work and should be considered co-first authors

* Corresponding author: qingyang_lin@zju.edu.cn; xgao1@zju.edu.cn

ABSTRACT

Massive emission of multi-pollutants from the utilization of fossil fuels has caused severe environmental problems in past decades. The transport process of multi-pollutant molecules in nano-porous materials is involved, and considered to be one of the most significant processes, in the removal of these pollutants no matter by adsorption or catalysis. However, the mechanism of nano-scale transport is not fully understood due to the complexity in pore structures and diversity in pollutants. This work probes into the application of non-equilibrium molecular dynamics (NEMD) simulations to study the mass transfer of multi-pollutants at nano-scale. A dual control-volume (DCV) model of titanium-based nanopore is proposed and molecules of NO, NH₃ and SO₂, which are typical gaseous species in selective catalytic reduction (SCR) process for nitrogen oxides removal, are investigated. Simulations are performed to investigate the influences of temperature, pore width and hydroxyl site on diffusivity of objective molecules. The results show (1) the differential transport of NO, NH₃ and SO₂ in various temperature and pore conditions, (2) the impact of OH-groups on diffusion in different pore widths, (3) the influence of competitive diffusion of NH₃ and SO₂. These

fundamental researches have provided guidance on the rational design of SCR catalysts for high deNO_x activity and low SO₂ oxidation.

Keywords: Molecular dynamics, Gaseous molecules, Multi-pollutant, Nanopore transport, Diffusivity

1 Introduction

Process of molecules transport in porous materials at nano-scale widely exists in a variety of scientific fields such as energy, environment and chemical engineering [1-3]. Studies on mass transfer in nanopores have played an important role in the advances in many applications, including heterogeneous catalysis, shale-gas exploitation, membrane separation, greenhouse gas capture [4-8]. There have been various experimental studies on novel ordered or hierarchical porous structures to optimize diffusion process and improve the performance of materials [9-12]. However, it is still challenging to obtain insights of the mechanism in nanopore diffusion by experiments due to the complexity in the structure of porous materials.

Therefore, computational methods have been utilized for better understanding of the transport behavior in order to further assist enhancing the design of porous materials for better diffusion. For

example, Jiao et al. [13] built a double-layer model with graphene membranes and simulated the interlayer diffusion of different molecules ($\text{CO}_2/\text{CH}_4/\text{N}_2/\text{O}_2/\text{CO}/\text{CO}_2/\text{H}_2\text{O}$) to study the trade-off between permeability and selectivity; Jiang et al. [14] modified a silicon atomic nano-channel with different wall roughness to figure out its influence on the methane flow; Sastre et al. [15] established a model of silicalite crystal to study the surface and intracrystalline diffusional resistance on benzene molecules; Further studies are still required in following aspects: firstly, the current works mainly focus on the conventional molecules in air but lack of attentions on multiple pollutants from industrial processes; secondly, there are limited works in the literature systematically studying the influences of pore structures on the diffusion (e.g. pore size, distribution, connectivity, etc.); thirdly, self-diffusion is the main interest of many works without taking the influences of pressure and chemical gradient into consideration.

In this work, we have developed a dual control-volume (DCV) model to simulate the diffusion process for gaseous molecules in a nano-scale pore. This method was firstly proposed by Heffelfinger et al. [16] to estimate the diffusivity of a steady flow by inserting GCMC (grand canonical Monte Carlo) process in standard NVT (constant particle number, volume and temperature) molecular dynamics simulation to randomly create and destruct particles in upstream and downstream control-volumes in order to set up a steady gradient between the two control-volumes and evaluate the diffusivity by Fick's law. However, the Monte Carlo process can be time-consuming considering that the aspects of GCMC part will not scale well in parallel when it comes to the full energy option in calculations. Therefore, alternative methods were investigated by considering nonequilibrium states in this work to save computing time from Monte Carlo process while typical DCV-GCMD simulations were still performed as comparisons. Molecules of NO, NH_3 and SO_2 from selective catalytic reduction (SCR) process, which is one of the most widely used

technologies for deNOx from industrial flue gas [17-21], were selected as guest molecules. Thereby, the transport of NO, NH_3 and SO_2 in titanium-based nanopore with different combinations of gas molecules, temperatures, pore widths and hydroxyl conditions were investigated with MD simulations and the results were analyzed to figure out the sensitivity of diffusivity, the impact of hydroxyl groups and the influence of multi-type molecules on diffusion.

2 Methods

2.1 Modeling of TiO_2 Nanopore

A three-dimensional model of titanium-based nanopore was established in this work to investigate mass transport behavior for different gaseous molecules at nano-scale. Simulations were carried out with pure and hydroxyl-functionalized pores of 25, 50 and 75 Å width. As shown in Fig.1, two $100\text{Å} \times 100\text{Å}$ control-volumes were set at the front and back of a 300Å long transport region. The rigid wall of transport region consisted of five layers of atoms from titanium dioxide and OH-groups with a certain density were introduced to hydroxyl-functionalize the pore. A periodic boundary condition was applied in the z direction.

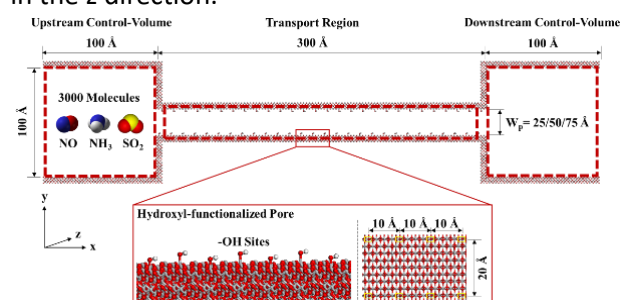


Fig.1. Modeling of titanium-based nanopore

2.2 Computational Method

In the MD simulation, intermolecular interactions were modeled with the combination of Lenard-Johns (LJ) potential and Coulomb potential while intramolecular potential energy of bond and angle in harmonic expressions was taken into consideration. All interactions were truncated at 10Å . Detailed potential parameters are shown in Table.1.

The system was firstly progressed for 0.5ns without removing the confinement between upstream control-volume and transport region to reach a pre-equilibrium stage and then a 3ns NVT simulation was performed with a time step of 2×10^{-3} ns. As for the cases with GCMC method applied,

insertion and deletion of molecules were performed every 5×10^{-4} ns during the NVT process to maintain a constant pressure of 50 and 10 atm for up and downstream control-volume. All the simulations were performed with the LAMMPS package.

Table.1. Detailed parameters for LJ and Coulomb potential.

Molecular	Element Symbol	Charge (e)	Parameters for LJ Potential		Molecular Topography	
			ϵ (kcal/mol)	σ (Å)		
NO	N	+0.029	0.158	3.014	N-O bond:	1.151Å
	O	-0.029	0.193	2.875		
NH ₃	N	-1.020	0.170	3.420	N-H bond:	1.014Å
	H	+0.340	0	0	H-N-H angle:	102.611°
SO ₂	S	+0.468	0.290	3.615	S-O bond:	1.431Å
	O	-0.234	0.114	3.005	O-S-O angle:	118.753°

2.3 Determination of Diffusivity

The advantage of using a dual control-volume model is to investigate diffusion process and obtain diffusivity from direct measurement of number of molecules. A time dependent distribution profile (or density profile) for guest molecules can be generated from simulation results, in which the actual number of molecules at any position and time step in the system can be tracked and analyzed.

2.3.1 Determination of diffusivity using Fick's first law

By applying Monte Carlo process to maintain a constant pressure gradient between up and downstream control-volume, a steady state flow will be developed and a direct measurement of diffusivity is allowed by calculating the time averaged density profile and flux. The diffusivity of component i can be determined by Fick's first law:

$$J_i = -D_i \frac{\partial \rho_i(x)}{\partial x} \quad (1)$$

where J_i is the time averaged flux, D_i the diffusivity, ρ_i the density for component i .

2.3.2 Determination of diffusivity using Fick's second law

Differing from the cases with steady state flow, the diffusivity in NVT cases has to be determined with the time-dependent density profile of molecules in all the regions by Fick's second law:

$$\frac{\partial \rho_i(x, t)}{\partial t} = -D_i \frac{\partial^2 \rho_i(x, t)}{\partial x^2} \quad (2)$$

where D_i is the diffusivity, ρ_i the time-dependent density for component i . It can be expressed as follow considering the scheme of dual control-volume model:

$$\frac{\partial \rho_i(x, t)}{\partial t} = \frac{\partial N_{D_i}(t)}{V \partial t} \quad (3)$$

$$-D_i \frac{\partial^2 \rho_i(x, t)}{\partial x^2} = -D_i \frac{N_{D_i}(t) - N_{U_i}(t)}{VL^2} \quad (4)$$

$$N_{U_i} + N_{T_i} + N_{D_i} = N_{Total} \quad (5)$$

where N_{U_i} , N_{T_i} , and N_{D_i} are the numbers of molecular i in upstream control-volume, transport region, and downstream control-volume, respectively; N_{Total} is the total number of molecular i used in the entire domain; L is the length of transport region; V is the size of the control-volume. We can then get:

$$\frac{\partial N_{D_i}(t)}{V \partial t} = -\frac{2D_i}{VL^2} \cdot N_{D_i}(t) + \frac{(N_{Total} - N_{T_i}(t))D_i}{VL^2} \quad (6)$$

where V , L are known constant parameters. N_{T_i} can be considered as a constant value after reaching the molecular capacity of transport region and obtained by linear fitting the time-dependent molecular quantity in transport region. Equation (6) can be solved as:

$$N_{D_i}(t) = \quad (7)$$

$$\frac{1}{p_1} e^{p_1(t-p_2)} + \frac{N_{Total} - N_{T_i}}{2}$$

$$D_i = -p_1 \frac{L^2}{2} \quad (8)$$

where parameter p_1 and p_2 can be obtained by fitting the time-dependent molecular quantity in downstream control-volume N_{D_i} .

Fig.2 shows an example of NO transport in 25Å hydroxyl-functionalized pore at 250°C to illustrate the determination of diffusivity with this method. Note that the diffusion process from 0.8 to 1.8ns holds a relatively constant number of molecules in the transport region of 744 and the fitting result for diffusivity turns out to be $217.1 \times 10^{-9} \text{m}^2/\text{s}$ with a R-square up to 0.9901, indicating the effectiveness of this method.

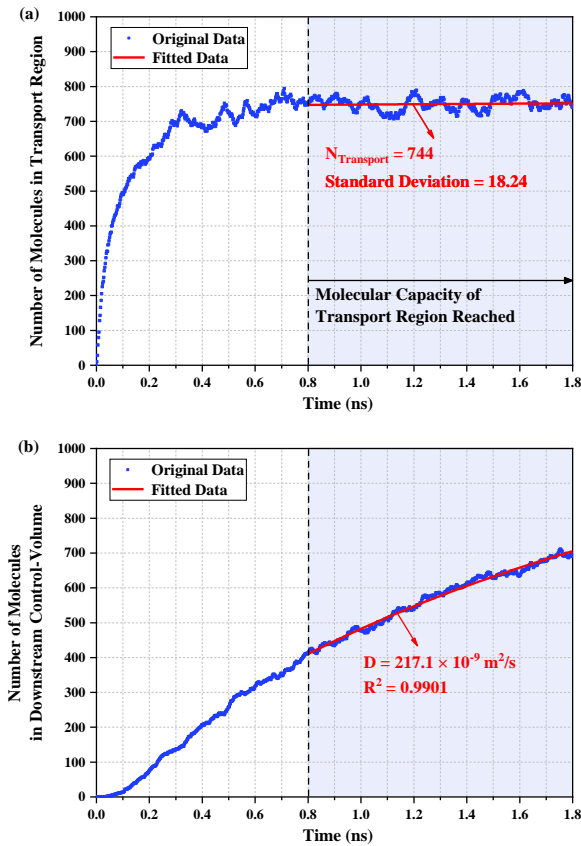


Fig.2. Determination of diffusivity for NO in 25Å hydroxyl-functionalized pore at 250°C: (a) determination of the number of molecules in the transport region $N_{Transport}$, (b) determination of diffusivity D .

3 Results and Discussions

3.1 Impact of Temperature and Hydroxyl Groups

Diffusivities for different molecular types vary to their properties such as molecular weight, dipole moment and dynamic diameter. They also make different responses to the changes in external factors such as

temperature and pore structures. In this section, 3000 molecules of NO, NH₃ and SO₂ were studied in the simulations with same pore width of 25Å but with temperature range from 150 to 450°C and different distributions of hydroxyl groups (-pure for pore without hydroxyl groups, -OH for pore with hydroxyl groups). All the diffusivities were calculated and averaged over one thousand time-steps to quantify the uncertainties. The computed diffusivity values at different conditions with standard deviations are plotted in Fig.3.

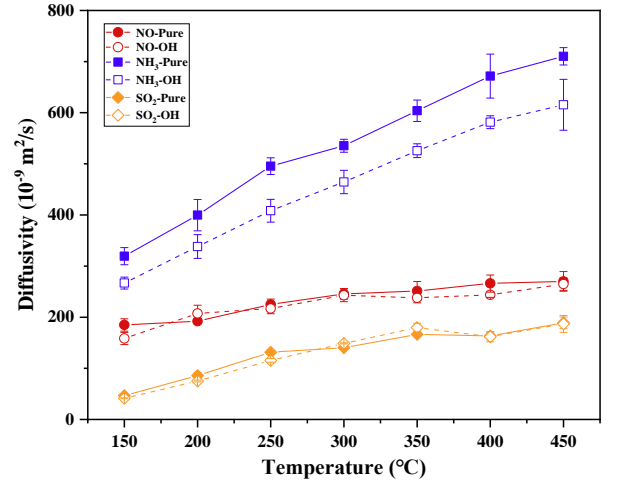


Fig.3. Diffusivities of NO/NH₃/SO₂ in 25Å pore with different temperatures and pore conditions.

As shown in the figure, the diffusivity for NH₃ is generally higher, covering a wide range of temperatures, followed by NO and SO₂. In the pore without any OH-groups (NH₃-Pure), the diffusivity of NH₃ increases from 319.5×10^{-9} to $710.3 \times 10^{-9} \text{m}^2/\text{s}$ when the temperature increases from 150 to 450°C. Meanwhile, in the pore with distributed OH-groups (functionalized with $0.005/\text{Å}^2$), the diffusivity of NH₃ increases from 266.8×10^{-9} to $615.5 \times 10^{-9} \text{m}^2/\text{s}$. It can be seen that the increase of temperature significantly enhances the diffusion of NH₃ molecules in 25Å pore while the existence of OH-groups slows it down, leaving an average difference up to 18.1% between the pure and hydroxyl-functionalized pore cases. However, temperature and OH-groups have less impact on the diffusivities of NO and SO₂. In the pure pore cases, the diffusivities for NO and SO₂ increase from 184.8×10^{-9} to $270.1 \times 10^{-9} \text{m}^2/\text{s}$ and from 46.7×10^{-9} to $188.9 \times 10^{-9} \text{m}^2/\text{s}$ respectively as the temperature grows. For cases with OH-groups, NO diffusivity increases from 158.4×10^{-9} to $264.9 \times 10^{-9} \text{m}^2/\text{s}$ and SO₂ diffusivity increases from 41.4×10^{-9} to $186.9 \times 10^{-9} \text{m}^2/\text{s}$. It can be inferred that NH₃ molecules are more likely to be attracted and slowed down by the OH-groups due to

their smaller molecular weights and stronger polarity comparing to NO and SO₂ molecules.

3.2 Effective Distance for Hydroxyl's Impact

The existence of OH-groups in the transport region may significantly slow down the diffusion of gaseous molecules in the pore because of the intermolecular interaction between OH-groups and gaseous molecules. However, according to the calculation of van der Waals and Coulomb potential energy, this slow-down effect will decline rapidly as the distance between the two species increases. Meanwhile, indirect drag effect from OH-groups also reflects on the collision of attracted molecules with those beyond the cut-off radius. Hence, the pore width has become an important factor influencing OH-groups on molecular diffusion, especially for NH₃. And it can be expected that a certain decrease in OH-groups' impact will be observed as the pore width increases. To further investigate the effective distance of OH-groups' impact, several simulations were performed on pores with different widths. 25, 50 and 75Å pore with a higher OH-group coverage of 0.01/Å² at 300°C were employed in the cases.

The diffusivities for these cases are shown in Fig.4. In the 25Å cases, the diffusivity in pore without any OH-group is measured as 535.4×10⁻⁹m²/s and the diffusivity in hydroxyl-functionalized pore is measured as 362.1×10⁻⁹m²/s, indicating a slowdown of 32.37% in diffusion at the presence of OH-groups. In the 50Å cases, the diffusivities of pure and hydroxyl-functionalized pore become 1255.4×10⁻⁹m²/s and 1147.1×10⁻⁹m²/s with the slowdown decreased to 8.62%. Furthermore, in the 75Å cases, the diffusivities are 2525.7×10⁻⁹m²/s and 2450.6×10⁻⁹m²/s respectively and the slowdown is merely 2.97%. It can be inferred that at somewhere between 50 and 75Å, the diffusivity difference between pure and hydroxyl-functionalized pore is lower than 5%, and in another word, hydroxyl groups cannot sufficiently affect the transport of NH₃ in these occasions.

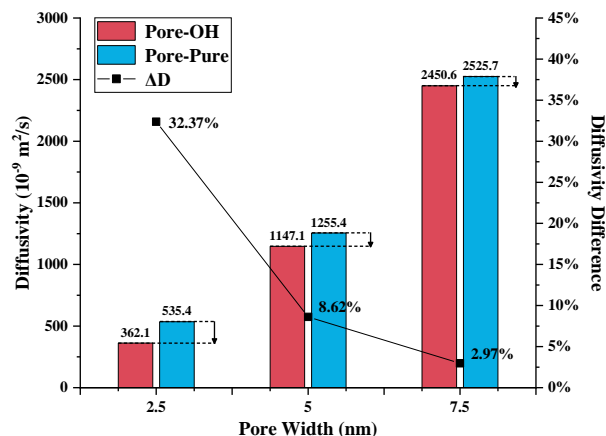


Fig.4. Impact of hydroxyl groups on NH₃ diffusivity in 25/50/75Å pore at 300°C.

3.3 Transport of Mixed Molecules

In practical industry processes, the component of flue gas could be complex and the competitive transport between different pollutants may take place in a single nanopore. To qualify the diffusivities under the impact of competitive transport, simulations with a mixture flow of NH₃ and SO₂ were performed in different conditions. 1500 molecules of both NH₃ and SO₂ were used for to maintain the constant total number of 3000 in all cases. The pore is 25Å with 0.01/Å² OH-groups and the temperature is 300°C.

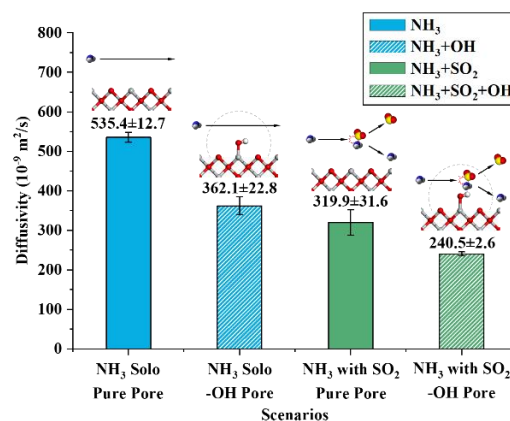


Fig.5. Impact of mixed molecules on NH₃ diffusivities in 25Å pore at 300°C.

The results with deviations for solo and mixed diffusion in 25Å pure and hydroxyl-functionalized pore at 300°C are shown in Fig.5. It can be seen that the diffusivity decreases from 535.4×10⁻⁹ to 319.9×10⁻⁹m²/s due to the introduction of SO₂. It can be inferred that the collision with molecules with greater weight, which are SO₂ in this case, has significantly inhibited the diffusion of NH₃, leading to a slowdown up to 40.3% in the scenario of equal partial pressure for NH₃ and SO₂. And

at the presence of both SO₂ and OH-groups, the diffusivity of NH₃ will be further reduced to 240.5×10⁻⁹m²/s. It is also worth noting that the introduction of OH-groups can reduce the diffusivity of NH₃ by 32.37% (from 535.4×10⁻⁹ to 362.1×10⁻⁹m²/s) in solo flow but only cause a slowdown of 24.82% (from 319.9×10⁻⁹ to 240.5×10⁻⁹m²/s).in mixed flow. This is because the insensitivity of SO₂ to OH-groups has weakened the impact of OH-groups on mixed flow through the intermolecular collisions. In conclusion, the attraction of surface sites and intermolecular collision are the two major influences in the competitive diffusion of mixed molecules. Molecules of smaller weight and stronger polarity are easily affected by surface sites when transport solo yet become less affected due to its collision with molecules of larger weight and weaker polarity in a mixed flow and vice versa.

4 Conclusions

In this study, we proposed a dual control-volume model for studying the transport behavior of different gaseous molecules in nanopores and quantifying the diffusivity. NO/NH₃/SO₂ in titanium-based nanopores were investigated. The results highlight the importance of factors such as temperature, pore width and hydroxyl groups in the diffusion process. The conclusions are:

1) The increase of temperature and pore width can enhance the diffusion while the introducing of hydroxyl groups will slow it down. The sensitivity of diffusivity to these factors varies with the type of molecular. It is shown that NH₃ is more likely affected by the temperature and hydroxyl groups in the pore than NO and SO₂ due to its stronger dipole moment and less molecular weight.

2) The impact of OH-groups on the diffusion of NH₃ declines rapidly as the growth of pore width. At a certain pore width between 50 and 75Å, the difference between NH₃ diffusivities of pure and hydroxyl-functionalized pore is less than 5%, indicating that OH-groups distributed on pore wall cannot effectively slow down the diffusion of NH₃ from this distance.

3) The impact of multiple factors on diffusion reflects in two aspects: one is to directly affect the intermolecular interactions within cut-off radius; the other is indirect, such as the collision and block between faster and slower types of molecules. And the latter is the main reason causing less sensitivity of NH₃ and more

sensitivity of SO₂ to the presence of OH-groups in mixed diffusion.

Acknowledgements

This work was supported by National Natural Science Foundation of China (No. 51836006, No. 52006192).

References

- [1] Yu, H., et al., Multiscale transport mechanism of shale gas in micro/nano-pores. *International Journal of Heat and Mass Transfer*, 2017. 111: p. 1172-1180.
- [2] Zhong, J.W., et al., Recent advances of the nano-hierarchical SAPO-34 in the methanol-to-olefin (MTO) reaction and other applications. *Catalysis Science & Technology*, 2017. 7(21): p. 4905-4923.
- [3] Epstein, I.R. and B. Xu, Reaction-diffusion processes at the nano- and microscales. *Nature Nanotechnology*, 2016. 11(4): p. 312-319.
- [4] Wang, H., et al., Modeling of multi-scale transport phenomena in shale gas production — A critical review. *Applied Energy*, 2020. 262: p. 114575.
- [5] Guo, Y., et al., Recent advances in VOC elimination by catalytic oxidation technology onto various nanoparticles catalysts: a critical review. *Applied Catalysis B: Environmental*, 2021. 281: p. 119447.
- [6] Shehzad, N., et al., A critical review on TiO₂ based photocatalytic CO₂ reduction system: Strategies to improve efficiency. *Journal of CO₂ Utilization*, 2018. 26: p. 98-122.
- [7] Zhou, L., et al., Recent Developments on and Prospects for Electrode Materials with Hierarchical Structures for Lithium-Ion Batteries. *Advanced Energy Materials*, 2018. 8(6): p. 1701415.
- [8] Bruno, G., et al., Unexpected behaviors in molecular transport through size-controlled nanochannels down to the ultra-nanoscale. *Nat Commun*, 2018. 9(1): p. 1682.
- [9] Md Jani, A.M., D. Losic, and N.H. Voelcker, Nanoporous anodic aluminium oxide: Advances in surface engineering and emerging applications. *Progress in Materials Science*, 2013. 58(5): p. 636-704.
- [10] Na, K., M. Choi, and R. Ryoo, Recent advances in the synthesis of hierarchically nanoporous zeolites. *Microporous and Mesoporous Materials*, 2013. 166: p. 3-19.
- [11] Wang, C., J.L. Wang, and W. Lin, Elucidating molecular iridium water oxidation catalysts using metal-organic frameworks: a comprehensive structural, catalytic, spectroscopic, and kinetic study. *J Am Chem Soc*, 2012. 134(48): p. 19895-908.

- [12] Wang, J.J., et al., Experimental investigation of gas mass transport and diffusion coefficients in porous media with nanopores. *International Journal of Heat and Mass Transfer*, 2017. 115: p. 566-579.
- [13] Jiao, S. and Z. Xu, Selective gas diffusion in graphene oxides membranes: a molecular dynamics simulations study. *ACS Appl Mater Interfaces*, 2015. 7(17): p. 9052-9.
- [14] Jiang, C., et al., The effects of wall roughness on the methane flow in nano-channels using non-equilibrium multiscale molecular dynamics simulation. *Microfluidics and Nanofluidics*, 2017. 21(5).
- [15] Sastre, G., J. Kärgler, and D.M. Ruthven, Molecular Dynamics Study of Diffusion and Surface Permeation of Benzene in Silicalite. *The Journal of Physical Chemistry C*, 2018. 122(13): p. 7217-7225.
- [16] Heffelfinger, G.S. and F.v. Swol, Diffusion in Lennard-Jones fluids using dual control volume grand canonical molecular dynamics simulation (DCV-GCMD). *The Journal of Chemical Physics*, 1994. 100(10): p. 7548-7552.
- [17] Gholami, F., et al., Technologies for the nitrogen oxides reduction from flue gas: A review. *Sci Total Environ*, 2020. 714: p. 136712.
- [18] Han, L., et al., Selective Catalytic Reduction of NO_x with NH₃ by Using Novel Catalysts: State of the Art and Future Prospects. *Chem Rev*, 2019. 119(19): p. 10916-10976.
- [19] Meng, D., et al., Spinel structured Co₂MnO₄ mixed oxide catalyst for the selective catalytic reduction of NO_x with NH₃. *Applied Catalysis B: Environmental*, 2018. 221: p. 652-663.
- [20] Janssens, T.V.W., et al., A Consistent Reaction Scheme for the Selective Catalytic Reduction of Nitrogen Oxides with Ammonia. *ACS Catalysis*, 2015. 5(5): p. 2832-2845.
- [21] Liu, Z., et al., Novel Mn-Ce-Ti mixed-oxide catalyst for the selective catalytic reduction of NO_x with NH₃. *ACS Appl Mater Interfaces*, 2014. 6(16): p. 14500-8.